

Laboratory observations of mean flows under surface gravity waves

S. G. MONISMITH^{1,4}, E. A. COWEN²,
H. M. NEPF³, J. MAGNAUDET⁴ AND L. THAIS⁵

¹Environmental Fluid Mechanics Laboratory, Stanford University Stanford, CA 94305-4020, USA

²Department of Civil and Environmental Engineering Cornell University, Ithaca, NY 14853, USA

³Parsons Laboratory, MIT, Cambridge MA 02139, USA

⁴Institut de Mécanique des Fluides de Toulouse, UMR-CNRS-INPT-UPS 5502, Toulouse 31400, France

⁵Laboratoire de Mécanique de Lille, UMR-CNRS 8107, Polytech'Lille, Université de Lille I,
Villeneuve D'Ascq, Cedex 59655, France

(Received 21 October 2005 and in revised form 2 August 2006)

In this paper we present mean velocity distributions measured in several different wave flumes. The flows shown involve different types of mechanical wavemakers, channels of differing sizes, and two different end conditions. In all cases, when surface waves, nominally deep-water Stokes waves, are generated, counterflowing Eulerian flows appear that act to cancel locally, i.e. not in an integral sense, the mass transport associated with the Stokes drift. No existing theory of wave–current interactions explains this behaviour, although it is symptomatic of Gerstner waves, rotational waves that are exact solutions to the Euler equations. In shallow water ($kH \approx 1$), this cancellation of the Stokes drift does not hold, suggesting that interactions between wave motions and the bottom boundary layer may also come into play.

1. Introduction

In his original work on water waves, Stokes (1847) discovered an interesting and significant property of the waves that now bear his name. To lowest order in wave slope, $\varepsilon = ak$ (a is wave amplitude and k is the wavenumber), the potential solution for water waves involves orbits that, at $O(\varepsilon^2)$, are not closed (see Kinsman 1984). For deep-water waves ($kH \gg 1$; H = fluid depth), this results in a net forward motion of fluid particles known as the Stokes drift, which can be approximated:

$$U_S = \varepsilon^2 \left(\frac{\sigma}{k} \right) \exp(2kz), \quad (1)$$

where σ is the angular frequency, given for deep-water waves by the dispersion relation (correct to $O(\varepsilon^2)$)

$$\sigma^2 = gk \quad (2)$$

and z is the vertical position measured positive upwards from the mean water level (which is constant to $O(\varepsilon^2)$). If a constraint of zero net mass flux is imposed, a depth-independent retrograde mean Eulerian velocity, \overline{U}_E , i.e. the Eulerian velocity measured at any point and averaged over a wave period, must develop (cf. Swan 1990*b*), such that the change in \overline{U}_E induced by the waves is equal and opposite to the

depth average of the Stokes drift, i.e.

$$\overline{U_E} = -\frac{\varepsilon^2 C}{2kH} \quad (3)$$

where $C = (\sigma/k)$ = the phase velocity of the waves. Note that above and in what follows, we use an overbar to indicate mean variables, by which we imply variables that are averaged over a wave period to filter out the periodic perturbations due to the waves (see Andrews & McIntyre 1978). In their development of a comprehensive theory of wave–current interactions using the generalized Lagrangian mean (GLM) formulation, Andrews & McIntyre (1978) show that correct to $O(\varepsilon^3)$,

$$\overline{U_L}(z) = \overline{U_E}(z) + U_S(z), \quad (4)$$

where $\overline{U_L}$ is the mean Lagrangian velocity and U_S is given to $O(\varepsilon^3)$ for deep-water waves by (1).

Longuet-Higgins (1953) reconsidered Stokes' result, adding significant corrections for the mass transport velocity due to the effects of thin viscous boundary layers that do not disappear in the limiting case of zero viscosity. He showed that in a closed channel when a purely viscous solution is valid, i.e. when $a \ll \delta$, where $\delta = (\sigma/\nu)^{1/2}$ is the thickness of the wave boundary layer (ν is the kinematic viscosity of the fluid), a pressure-gradient-driven compensation flow is established that provides the retrograde mass flux required to preserve local mass conservation. Additionally, as a consequence of phase shifting of the vertical and horizontal velocities in the wave boundary layer, a net stress is felt by the Eulerian flow that increases the total net flow. In this case, vorticity enters the interior of the fluid by diffusion, presumably requiring a time of $O(H^2/\nu)$ to be established. However, Longuet-Higgins also pointed out that when $a > \delta$, vorticity could be transported into the interior of the fluid via horizontal advection by the mass transport velocity itself rather than by diffusion.

Russell & Osorio (1958) reported the results of laboratory experiments with mostly (although not exclusively) shallow-water waves in which the velocities derived from the displacements of small particles and dye lines. These compared favourably to predictions made using Longuet-Higgins' theory, with the agreement being best for viscous flows in the bottom boundary layer. The comparison of surface velocities was more equivocal, since for deep-water waves Russell & Osorio's measurements showed mean Lagrangian velocities approximately equal to the Stokes drift (cf. their figure 14). The problem with this result is that for a viscous flow with a contaminated surface (as described by Russell & Osorio, the surface was either dirty or covered with a surfactant that they had added to the flow), $\overline{U_L}$ should be as much as twice what is suggested by (1) (see e.g. Law 1999). Swan (1990*b*) carried out laboratory experiments aimed at testing the effectiveness of advection at establishing vortical mean flows under waves. His experiments demonstrated that contrary to all theoretical expectations, Eulerian mean flows with negative vorticity developed. He attributed this to backwards advection, presumably by the mean return flow, of vorticity from the beach upon which his waves broke and were dissipated (see Matsunaga, Takehara & Awaya 1994).

Swan is not alone in finding negatively sheared mean Eulerian flows below water waves. For example, in their work on wave–current interactions and bottom boundary-layer modification, Kemp & Simons (1982) observed reductions in the mean Eulerian velocity owing to the addition of waves onto turbulent channel flows. This reduction was strongest near the water surface and increased with increasing wave amplitude. Jiang & Street (1991) measured mean Eulerian flows that were in opposition to

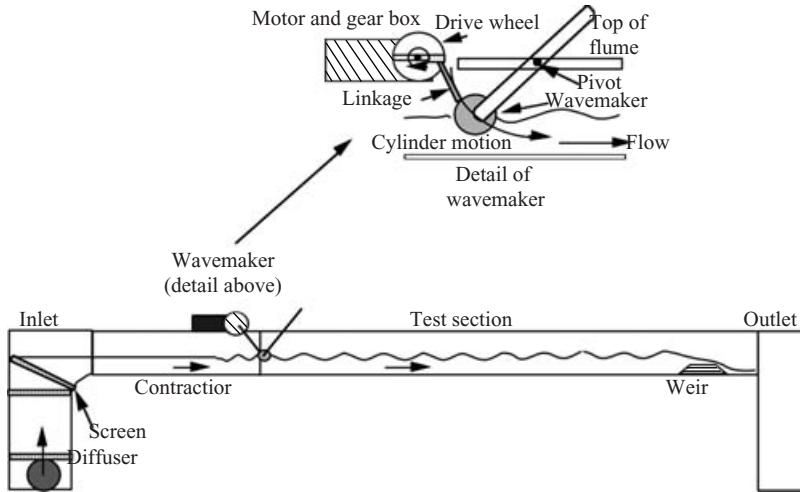


FIGURE 1. Sketch of the wave-current flume used by Nepf *et al.* (1995).

mechanically generated waves propagating down a large windwave flume with closed ends. They found that the negative Eulerian velocities appeared to compensate for the Stokes drift such that material lines (e.g. a dye line) did not deform as expected from Stokes' theory (J. Y. Jiang, personal communication 1990). Groeneweg & Klopman's (1998) theory of wave-current interaction (see also Groeneweg & Battjes 2003) also based on GLM theory but including turbulence and wave evolution, successfully predicted similar alterations to the mean flow by waves, as measured by Klopman (1994).

In the rest of this paper we discuss further observations of the type presented by Jiang & Street. We consider velocity measurements made in the wave flume described by Nepf *et al.* (1995). Some of these were made in the course of the experiments described by Nepf *et al.* (1995), and some were made later to specifically look at establishment of the mean flow. We also re-analyse the experimental data given in Jiang & Street (1991), Swan (1990*b*) and Thais (1994). In sum, these experiments find consistently that waves generated in various wave flumes do not alter the pre-existing Lagrangian mean flow.

2. Experiments with waves on a mean current

2.1. Experimental methods and facility

The first set of experiments we discuss were made in the flow-through wave flume at Stanford University used for the studies reported by Nepf (1992), Nepf & Monismith (1994) and Nepf *et al.* (1995). A sketch of this flume is given as figure 1. The test section of the flume is 1.2 m wide, 4.9 m long and typical flow depths for the results discussed herein was 10 cm. The depth in the channel is controlled by a broad-crested weir located at the downstream end of the channel. Because it is a hydraulic control, this weir also serves as a nearly-reflectionless beach. The superimposed flow enters the channel through a diffuser, rises vertically then passes through a 2:1 horizontal quintic contraction into the test section. In some experiments, a curved screen (designed according to Coehlo 1989) was used to create positive and negative velocity shear of approximately $\pm 1 \text{ s}^{-1}$ in the mean velocity profile outside the boundary layer. Typical mean flow velocities were 12 to 14 cm s^{-1} .

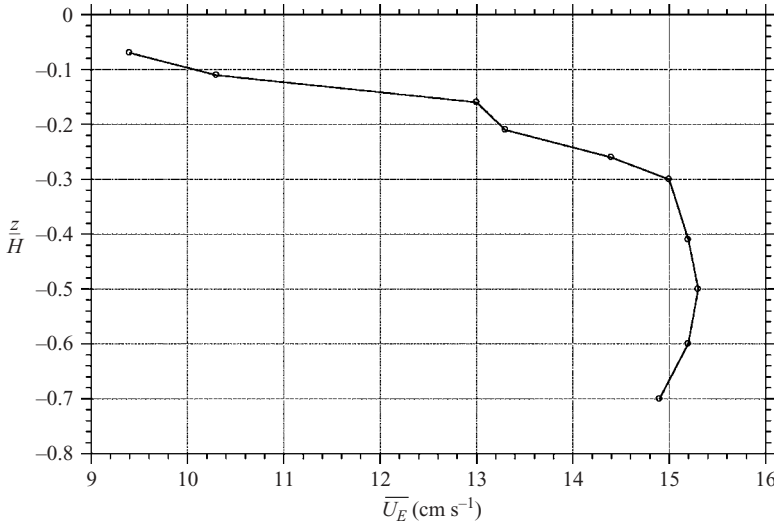


FIGURE 2. $\overline{U_E}$ measured 25 cm downstream of the wavemaker in the absence of waves (taken from Kimmel 1994).

The wavemaker used in this facility is comprised of an 85 mm diameter cylinder that is driven mechanically through a small arc by an electric motor. The mean submergence of the cylinder (typically 20 to 30 mm) and its stroke (range: 0 to 25 mm) are adjustable. The arc described by the cylinder entails a small degree of horizontal motion as well as vertical motion (it is not quite a piston) which causes the waves that it makes on the downstream side to be different from those on the upstream side. This wavemaker also serves to strip the surface film off the flow entering the channel.

For a range of 2 to 4 Hz, the waves made by the wavemaker appear to be Stokes waves in that their shapes can be described well by that of a Stokes second-order wave (Nepf & Monismith 1994). When $\varepsilon > 0.25$, the waves break (spilling-type breaking) continuously for four or five wavelengths as they leave the wavemaker (Nepf *et al.* 1995).

Eulerian velocities were measured to within 5 mm of the wave troughs 140 cm downstream of the wavemaker with one and two component laser-Doppler velocimeters (Nepf 1992). Lagrangian surface velocities were measured by timing the motions of 3 mm plastic particles floating on the water surface as they travelled from a point near the centre of the channel 1 m downstream of the wavemaker to a point 3 m downstream. Wave heights were measured with a standard single-wire capacitive wave height gauge (see e.g. Cheung & Street 1988).

2.2. Results: velocity measurements

The flow past the wavemaker generates a strong shear layer owing to separation of the flow behind the moving cylinder. A sample velocity profile measured 25 cm downstream of the wavemaker in the absence of waves is shown in figure 2 (taken from Kimmel 1994). However, this shear layer diffuses rapidly, relaxing to the velocity profiles shown below. Changes in time-averaged streamwise velocity owing to static

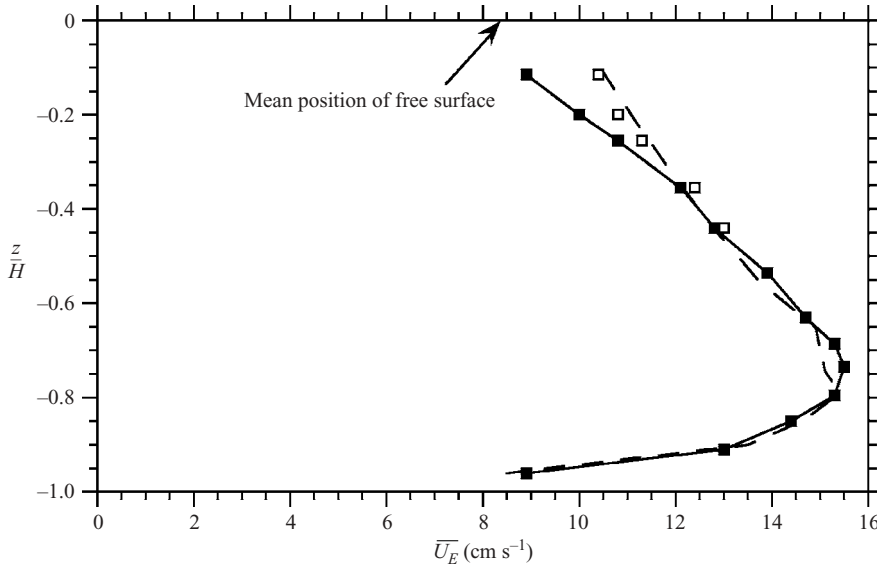


FIGURE 3. Effect of a wave ($f = 3.6$ Hz; $\varepsilon = 0.22$) on the Eulerian mean velocity profiles of a flow with an imposed negative shear. The profiles given are for ---, \overline{U}_E – no waves; ■, \overline{U}_E – flow with waves; □, \overline{U}_L – flow without waves.

changes in the wavemaker position, measured 5 mm below a flat surface, were within the range of variation found for the time-averaged streamwise velocity using 200 s averages.

The principal finding in this experiment is as follows. When non-breaking waves were imposed on the flow, the time-averaged Eulerian velocity was reduced near the surface. An example of this behaviour for a flow with an imposed negative shear of roughly 1 s^{-1} is given as figure 3. However, if we add the Stokes drift velocity at each depth (equation (1)) to produce \overline{U}_L , we recover the original mean Eulerian profile. As a consequence, as one should expect, the total mass transport, which is provided by pumps, is unaffected by the waves. However, this appears to hold in a pointwise rather than integral fashion.

To check the generality of the effect demonstrated in figure 3, we compare the measured change in the mean Eulerian velocity $\Delta\overline{U}_E$ for several conditions (both with and without negative imposed shears) to what one would predict if $\Delta\overline{U}_E = -U_S$ i.e. that \overline{U}_L was unaffected by the waves. Accounting for the effects of finite depth (e.g. Dean & Dalrymple 1991), the appropriate expression for U_S is:

$$\frac{U_S}{\varepsilon^2 C} = \frac{\cosh(2k(z+H))}{2 \sinh^2(kH)}. \quad (5)$$

The result of this comparison (figure 4) indicates that \overline{U}_L is indeed unaffected by the waves in this flow. This should be qualified: we have not included breaking waves in this comparison. Indeed, when the waves have broken, the near-surface shear is virtually eliminated (Nepf *et al.* 1995), implying changes in \overline{U}_L .

The hypothesis that \overline{U}_L remains constant up to the point of wave breaking can be assessed by examining Lagrangian velocities directly. For this we used floating

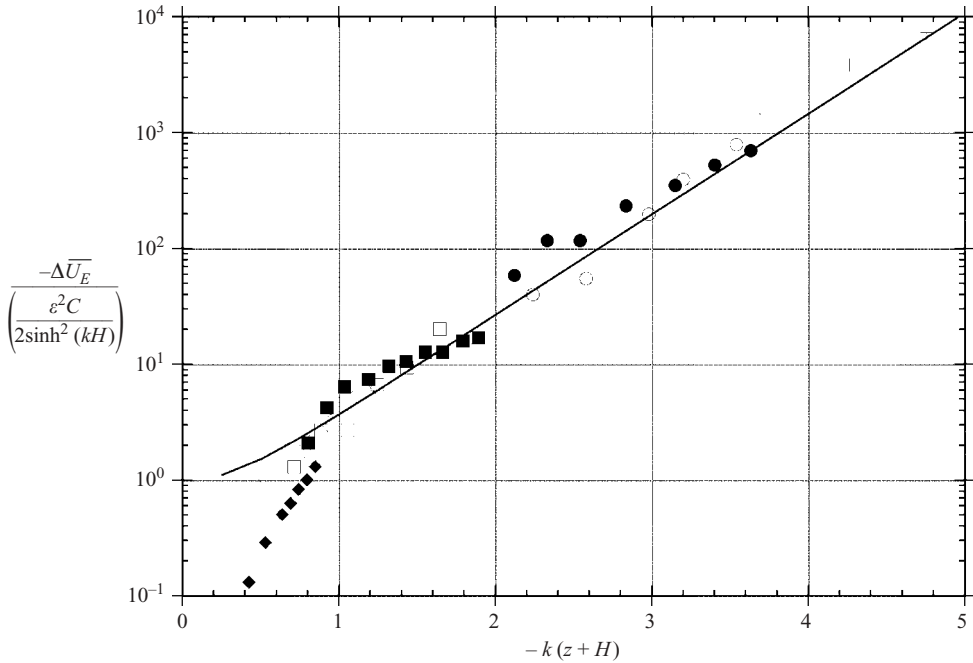


FIGURE 4. Effect of waves on mean flow $-\Delta \overline{U}_E$: —, assuming constancy of the Lagrangian mean velocity with U_S given by (5) and after the removal of the dependence on kH ; \circ , $kH = 4$, $\varepsilon = 0.25$; \square , $kH = 1.9$, $\varepsilon = 0.14$; \diamond , $kH = 1.5$, $\varepsilon = 0.16$; \times , $kH = 1.4$, $\varepsilon = 0.19$; and $+$, $kH = 5.3$, $\varepsilon = 0.22$; \bullet , $kH = 4.2$, $\varepsilon = 0.25$ (no imposed shear); \blacksquare , $kH = 2.2$, $\varepsilon = 0.22$ (no imposed shear); \blacklozenge , $kH = 1.04$, Klopman (1994) wave on co-flowing current.

particles. Figure 5 shows the surface velocity measured for one wave frequency (3.24 Hz), and a sequence of different amplitudes, expressed as wave slopes (ε). To calculate k , we used the Doppler-shifted dispersion relation

$$\sigma = \sqrt{gk \tanh(kH)} + \overline{U}_E k. \quad (6)$$

We have also included a plot of the surface value of \overline{U}_L calculated assuming that the Eulerian flow remains unchanged. As seen in figure 5, the constancy of \overline{U}_L at the surface (at least up to breaking) is clear.

2.3. An unsteady experiment

It is possible that negative vorticity can be produced on the wavemaker in order to satisfy the flow condition that \overline{U}_L be equal to the mean velocity of the wavemaker (Andrews & MacIntyre 1978), i.e. that $\overline{U}_L = 0$ there. This vorticity could then be advected from the wavemaker by any downstream mean flow. This would correspond to Longuet-Higgins' (1953) convection solution. If we were to start the wavemaker, then we would expect that this vorticity would arrive at a given distance downstream of the wavemaker in a time determined by the advection of that vorticity by the mean flow.

To test this idea we carried out a simple experiment in the large wave-current facility described in Cowen, Monismith & Koseff (1996). On the back wall of the inlet section, this flume has a wavemaker that operates effectively like a hinged plate; it was designed to minimize flow disturbance. The simple experiment we carried out

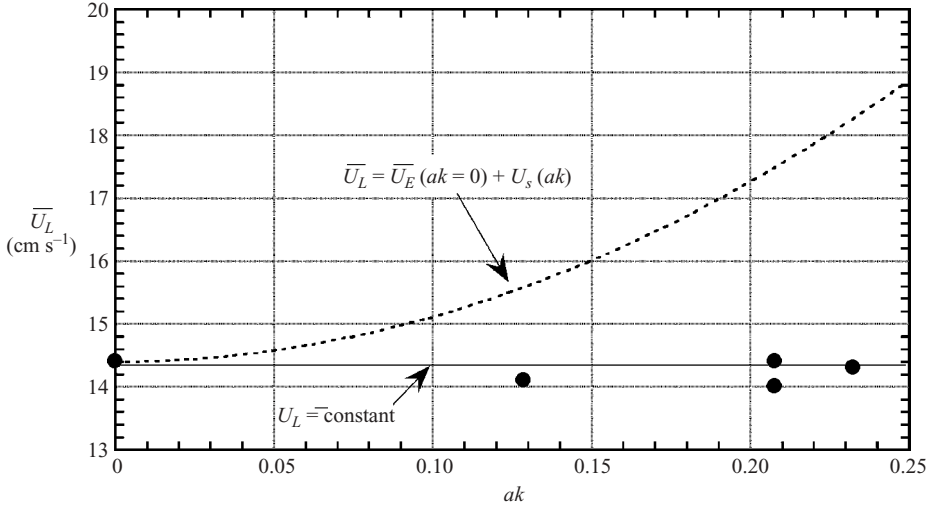


FIGURE 5. \overline{U}_L at $z=0$ as a function of wave steepness (ak): \bullet , measured ($f = 3.42$ Hz, $\overline{U}_E = 14.5$ cm s $^{-1}$ and $H = 10$ cm); $-$, assuming that $\overline{U}_L = \overline{U}_E$ as measured in the absence of waves and \cdots , assuming that \overline{U}_E is unchanged by the waves.

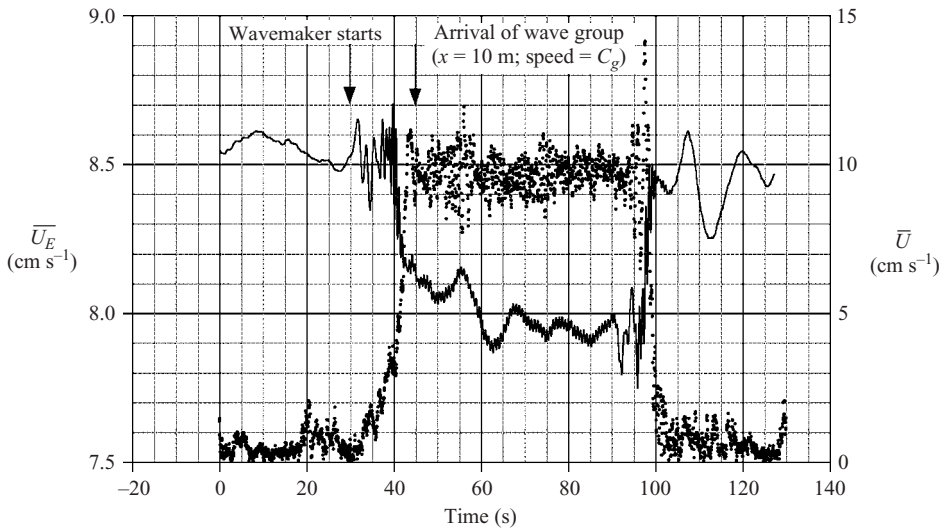


FIGURE 6. $-$, \overline{U}_E and \square , horizontal component of wave orbital velocity \tilde{U} associated with transient wave generation in a flume with a mean current (see text for full description of wave and flow conditions).

was to start the wavemaker, record the change in flow as the waves arrived, and then stop the wavemaker. Because the mean flow was turbulent, we repeated this transient wave generation 150 times and then ensemble averaged the low-pass filtered flows that resulted. We present one example of this behaviour for which $k = 0.072$ cm $^{-1}$, $\varepsilon = 0.1$, $kH = 2.1$, $C = 122$ cm s $^{-1}$, and $\overline{U}_E = 8.5$ cm s $^{-1}$ without waves, although we made several similar tests.

In figure 6, we plot one realization of the time-varying wave amplitude, calculated using the Hilbert transform (cf. Melville 1983), and the ensemble-averaged low-pass

filtered velocity, both determined using a one-component laser-Doppler anemometer (LDA) positioned 48 mm below the at-rest free-surface position approximately 10 m downstream of the wavemaker. At this depth, based on the observations above, we expect a reduction of approximately 6 mm s^{-1} . The mean velocity shows damped long-wave oscillations, and the expected reduction. Most importantly, the reduction arrives and leaves with the waves: the advection time for vorticity is predicted to be roughly 120 s, whereas the wave group should arrive 15 s after the wavemaker is started.

This type of behaviour of the mean flow is described in McIntyre (1981) who discusses the analysis of Longuet-Higgins & Stewart (1962) of wave group behaviour and radiation stresses. According to Longuet-Higgins & Stewart (1962), it is expected that an irrotational mean flow will be coincident with the waves. However, the depth scale for this slowly varying flow is the inverse of the width of the group in wavenumber space; i.e. if the energy of the group is contained in a band of wavenumbers of width Δk , the vertical scale of decay is found to be Δk^{-1} . In the present case, because the group is very long, the wave energy is confined to a very narrow range of wavenumbers (from spectra we find $\Delta k < 0.1k$), hence we should expect to see a nearly depth-independent flow, i.e. the mean velocity should be given by (3), namely 3 mm s^{-1} . This value clearly underpredicts the change in mean flow due to the waves. In contrast, the observed velocity reduction of roughly 6 mm s^{-1} is close to what one would calculate using (1), i.e. 6.1 mm s^{-1} .

Thus, the induced velocity difference near the surface is associated purely with the waves, and cannot be the result of (slow) advection of vorticity from the wavemaker or the far end of the tank. This behaviour is also consistent with the observations presented in §2.3 in that in the smaller flume, the wake of the cylinder manages to diffuse away leaving only the Stokes drift reduction in its place. However, since we have not directly measured vorticity, we cannot conclude that vorticity arrived with the waves. Instead, we can only say that a velocity change consistent with that which we observe for steady flows comes and goes with the waves. Given that the steady flows are rotational, it does seem possible that the unsteady flows are also rotational.

3. Experiments with wavemakers in closed channels

3.1. *The experiments of Jiang & Street (1991)*

These measurements were carried out in the 22 m long, 0.91 m wide wind-wave facility formerly located at Stanford. This facility included a hydraulically driven piston-type wavemaker that generated waves mechanically. Jiang & Street measured time-averaged profiles of the streamwise velocity under 1 Hz waves ($kH = 4$; $\varepsilon = 0.088$) using a single-component LDA. Their figure 2 is reproduced here as figure 7, although their data have been replotted so as to facilitate comparison with our hypothesis that $\overline{U}_E = -U_S$ in the presence of waves. As we found in the flowing channel, the mean Eulerian velocities, almost exactly cancel the Stokes drift, i.e. leading as before to $\overline{U}_L = 0$ at all depths.

3.2. *The experiments of Swan (1990b)*

These experiments were carried out in a wave tank at Cambridge University that 'is 0.6 m wide, 18.5 m long, and has a beach slope of 1:20', and had a piston-type wavemaker (Swan 1990). The waves he studied had $\sigma \approx 7 \text{ s}^{-1}$, $\varepsilon \approx 0.16$ and $kH \approx 1.8$. There was no imposed mean flow in these experiments. As Swan (1990) notes, breaking of the waves on the beach led to considerable three-dimensionality in the velocity

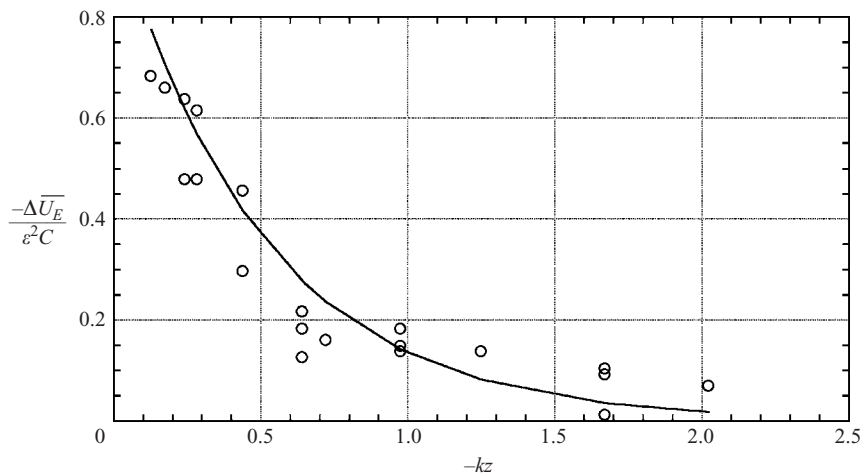


FIGURE 7. ○, Profiles of $-\overline{U}_E$ measured by Jiang & Street (1991) and —, U_S given by (5). Velocities have been normalized by $\varepsilon^2 C$.

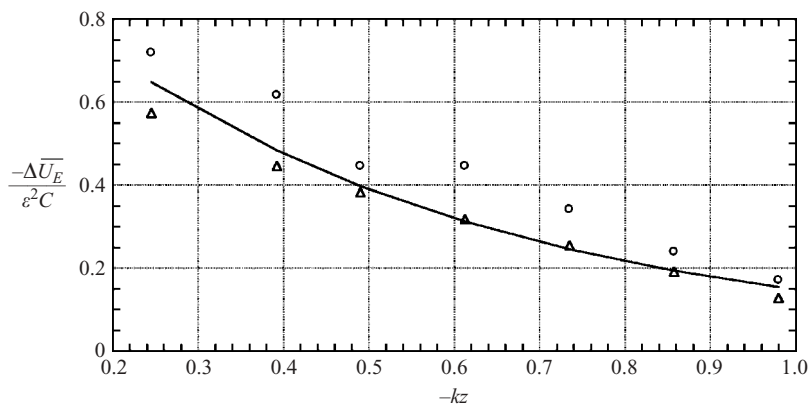


FIGURE 8. Profiles of $-\overline{U}_E$ measured by Swan (1990): ○, figure 2; △, figure 5(a) (with offset); and —, U_S given by (5). The dimensionless variables are the same as those in figure 7.

field near the beach (his figure 1), although all three profiles he gives, which were taken at different spanwise locations, show backflow and similar negative shears, i.e. that the backflow intensifies with height, much as the Eulerian deficit increases in the experiments discussed above.

In figure 8, we re-plot the other two full-depth profiles he gives (his figures 2 and 5a) with the profiles one would expect, given the constancy of \overline{U}_L , which in this case should be zero. The first profile was measured in the centre of the tank whereas the second was measured near to the beach. For the purposes of the comparison, we have subtracted a constant offset of 20 mm s^{-1} (approximately 55% of the surface Stokes drift velocity), the mean velocity observed near the bottom, from the second profile. While it is not clear why the mean velocity should be offset, the agreement of measurements and the prediction that $\overline{U}_E = -U_S$ is clearly quite good. In fact, if

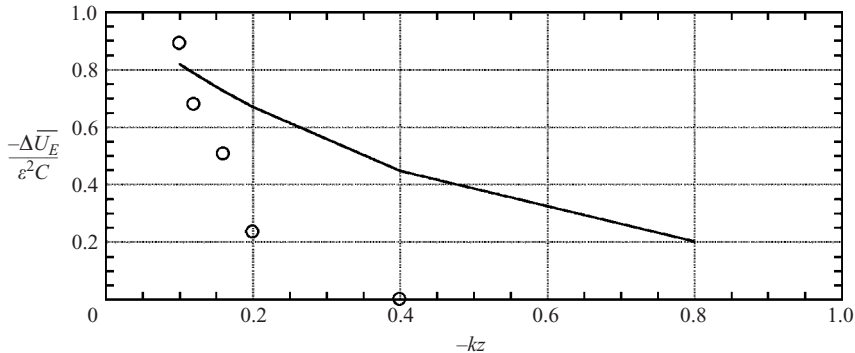


FIGURE 9. \circ , Profiles of $-\overline{U}_E$ measured by Thais & Magnaudet and $—$, U_S given by (5). The dimensionless variables are the same as those in figure 7.

offset by varying amounts between 10 and 30 mm s⁻¹, all of his measured profiles are similar to those shown above, i.e. $\overline{U}_E(z) = -U_S(z) + \text{constant}$.

3.3. *The experiments of Thais (1994)*

The last measurements we discuss are those made in the large wind-wave facility at IMST Luminy in Marseilles. This tank is 40 m long and 2.6 m wide. A water depth of 0.9 m was used for the experiments described by Thais (1994) in which he examined the effects of waves on wind-driven currents. Mean velocity measurements were made with a fibre-optic two-component LDA connected to spectrum-analyser-type ‘burst’ processors.

Figure 9 plots Thais’ (1994) data for a 1.0 Hz wave with $\varepsilon = 0.1$ in the absence of wind. These measurements were made after letting the wavemaker run for ~ 3 h. Again the strong backflow is seen near the surface, and as before, the time scale of advective establishment is too long, and the vorticity is of the opposite sign of that given by Longuet-Higgins’ viscous solution. In this case, the comparison between the measured velocity and the distribution of \overline{U}_E required for $\overline{U}_L = 0$ is not as good as in the two cases cited above. In particular, the return current decays more quickly over depth and is stronger than what would be predicted assuming that $\overline{U}_L = 0$ at all depths. Nonetheless, $\overline{U}_L = 0$ at the surface, and the trend and magnitude are similar to what would be expected assuming our hypothesis to hold.

4. Discussion

4.1. *Summary of the observations*

The measurements we present above show systematically that mechanically generated waves create mean Eulerian flows that are directed in the opposite direction to wave propagation. This result seems to hold with and without mean flows and with very different types of wavemakers and channel size. Considered from the standpoint of extant theory, it is even more surprising that the induced backflow can exactly cancel, at each depth, the mass transport associated with the Stokes drift. This effect does not appear to be associated with the transport of vorticity from the wavemaker, nor does it appear to result from diffusion, since there is no negative vorticity source

Reference	Type of flow	Flow	kH
Nepf <i>et al.</i> (various)	Open (pumped)	Turbulent	1.4 to 4
Cowen <i>et al.</i> (various)	Open (pumped)	Turbulent	2.1
Klopman (1994)	Open (pumped)	Turbulent	1.04
Jiang & Street (1991)	Closed (zero transport)	Laminar	4
Swan (1990)	Closed (zero transport)	Laminar	1.8
Thais & Magnaudet (1996)	Closed (zero transport)	Laminar	4

TABLE 1. Summary of experiments.

that can be identified (the surface boundary layer should contain positive vorticity – Longuet Higgins 1953, 1960, 1992). As a consequence, for these experimental flows, we conclude that $\overline{U_L}$ is little affected by the addition of waves. That is, the waves do not alter the ‘mean flow’ as seen from a Lagrangian perspective.

4.2. Comparison of observations with theory

How do these observations compare to existing theory? Groeneweg & Klopman (1998) extended the GLM model of Leibovich (1980) for wave–current interactions to include a wave-affected turbulence closure as well as for changes in wave amplitude due to damping of the waves. In their paper, comparison of this theory with observations made by Klopman (1994) for waves propagating with and against turbulent flows showed good agreement between predicted and observed velocity profiles.

Huang & Mei (2003) developed a similar analysis. They also predict near-surface reductions in the mean Eulerian flow for waves propagating with the current. Their analysis makes clear that in two dimensions, the key term available to change the mean flow profile is a depth-variable force that arises from the interaction of the vertical wave velocity and the wave-periodic vorticity (termed orbital vorticity by Magnaudet & Masbernat 1990). Huang & Mei show that when the periodic Reynolds stresses can be computed as the product of an eddy viscosity that is constant in time and the periodic (wave) velocity gradients, this body force is proportional to the curvature of the assumed eddy viscosity profile. Setting aside the issue that this form of turbulent closure may be inappropriate for wavy turbulent flows (Monismith & Magnaudet 1998; Teixeira & Belcher 2003), there is still the requirement that for this mechanism to work, the underlying flow must be turbulent. In contrast, the observations of reductions in Eulerian mean flow we report above took place in flows that were turbulent and in flows that were laminar, i.e. without respect to whether the flow was laminar or turbulent (see table 1). Thus, these observations suggest that the presence of turbulent stresses is not a necessary condition for vertical variations in the mean Eulerian flow to develop in the presence of waves.

An alternative analysis can be developed using the work by Mellor (2003) who extended classical radiation stress theory (Longuet-Higgins & Stewart 1962) to include vertical variations in mean flows interacting with waves. As shown in the Appendix, the mean Eulerian flow that is created should cancel the Stokes drift transport in an integrated fashion only, not pointwise as shown above. While consistent with the analysis of Longuet-Higgins & Stewart (1962, see also McIntyre 1981), this theory too does not explain the laboratory observations discussed above.

A different model for the waves that are created in the laboratory is one in which those waves have zero net particle displacements. If this is so, then negative mean Eulerian flows are a necessary consequence of the positive Stokes drift. They will be seen when the waves are present and will disappear as soon as the waves leave. It is well known that the Gerstner wave (Kinsman 1984), a periodic deep-water wave that exactly satisfies the free-surface dynamic and kinematic boundary conditions, has this property, i.e. it has closed orbits. To lowest order in ε , the Stokes and Gerstner waves are identical; however, at $O(\varepsilon^2)$, the Gerstner wave has a mean Eulerian flow

$$\overline{U_E} = -U_S,$$

i.e. exactly what we observe and have presented above.

Thus, given that the change in the Eulerian mean flow that accompanies Gerstner waves does not require that turbulence be present, it would appear that the Gerstner wave model provides a simple and accurate description of what we have observed in the laboratory. In a similar fashion, Gjøsund (2000, 2003) makes extensive comparisons between wave velocity predictions made using a generalization of Gerstner theory to arbitrary depth and time-varying amplitudes and observations made in a large laboratory wave tank. Again, the comparison is excellent, with the extended theory (which too does not include turbulence) consistently predicting the negative Eulerian mean velocities that develop when waves are present.

While the measurements we describe above conform well to the Gerstner model, there are examples of direct measurements of wave behaviour in the laboratory that appear to support the Stokes model. Notably, nine experiments with deep-water waves presented by the Beach Erosion Board (1941) show net particle displacements roughly in accord with (1) as modified to include a mean velocity such that the total horizontal drift is zero. A second feature of Gerstner waves that differs from that of Stokes waves is that their phase velocity and thus wavelength are independent of amplitude, whereas Stokes waves have a correction to phase velocity and thus wavelength that is second order in ε . While the Beach Erosion Board (1941) found the Gerstner model to be slightly better in predicting phase velocity and wavelength, both the Gerstner and Stokes models were within 1% of the measured values for both phase velocity and wavelength, an amount certainly likely to have been well within experimental error. Wiegel (1964) also presents measurements of wavelength dependence on amplitude; these too do not show the trends expected for Stokes waves, although again the changes in wavelength that must be measured are only a few per cent of the wavelength itself.

Most importantly, there is a well-known difficulty with Lagrangian waves such as the Gerstner waves: they are rotational (cf. Lamb 1932, art 251). This important point is puzzling because there does not appear to be any obvious explanation of how the vortical flow associated with the Stokes drift reduction is established, nor how it can propagate at the group velocity of the waves, in the case of time-varying amplitudes. In the case of the vortical boundary layers of the Stokes wave (Longuet Higgins 1992), vorticity is fluxed through the surface so as to maintain the zero stress (not zero vorticity) condition on the surface. Over a long time, this vorticity can be diffused through the fluid. However, this vorticity has the opposite sign to what we observe, and only enters the body of the fluid over the long times that characterize viscous diffusion. Thus, vorticity diffusion from the surface cannot be used to explain our observations, especially the transient behaviour noted in §2.4. Thus, while the Gerstner wave may be a viable kinematic explanation of our observations, the dynamical basis for the

development of the apparently rotational flows that we observe remains unresolved at present.

4.3. Effects of water depth

As shown in Gjørund (2000, 2003), Miche's (1944) extension of Gerstner's theory to periodic motions in finite depth predicts that $\Delta \overline{U}_E = -U_s(z)$ and thus that \overline{U}_L is constant even for values of $kH \approx 1$ or less. In contrast, while \overline{U}_L is constant for the experiments cited in §3, this behaviour does not hold for all such experiments reported in the literature. For example, neither Klopman's (1994) velocity profiles presented in Groeneweg & Klopman (1998) nor those of Kemp & Simons (1982) show constancy of \overline{U}_L . To illustrate this, in figure 4 we have also plotted Klopman's (1994) data in the same terms as we plotted our data. Klopman's data along with our results for the shallowest flows (in terms of kH) make clear that for shallow-water waves, i.e. $kH \approx 1$, \overline{U}_L is not constant. For example, the Klopman experiment has $kH = 1.06$, whereas the smallest value of kH for the other experiments shown in figure 4 was 1.4.

Given that the wave-current interaction theories of Huang & Mei (2003) and Groeneweg & Klopman (1998) largely depend on the $O(\varepsilon)$ perturbation velocity fields, and that these are identical for Stokes and Gerstner/Miche waves, it seems reasonable to hypothesize that as $kH \rightarrow 1$ (or less) the interaction of the surface wave with the bottom boundary layer becomes pronounced, thus altering the vertical variation of \overline{U}_L (although not its depth integral) in ways existing theory should describe.

4.4. Implications for ocean waves

It is important to note that all of the observations reported above were made in confined channels with mechanically generated waves (see also Gjørund 2000). Smith (2006) reported striking field observations of mean currents under wave groups measured in the open ocean, finding, as we do, that mean Lagrangian flows are unaltered by superimposed waves. Thus, we must conclude that the laboratory observations we report do not reflect some artefact of the laboratory but rather the real behaviour of some surface gravity waves.

From a practical standpoint, we note that an $O(\varepsilon^2)$ mean Eulerian flow does not affect any of the wave properties derived from the $O(\varepsilon)$ fluctuating wave velocities, e.g. radiation stresses (Longuet-Higgins & Stewart 1962) or the viscous boundary-layer flows described by Longuet-Higgins. However, it does complicate matters with respect to the nearshore transport of tracers or passive organisms (Monismith & Fong 2004): observations of currents must be corrected for the Stokes drift (e.g. per 5) whereas if \overline{U}_L is not changed by waves, *a priori* predictions of transport need not account for the waves at all, except to the extent that they modify bottom boundary-layer structure.

5. Conclusions

We have presented evidence gathered from several different experiments that waves generated mechanically in the laboratory do not change the Lagrangian mean velocity until they are sufficiently steep to break. In contrast to existing theory, this behaviour occurs whether or not the flow is turbulent and is present only when the waves are present. Smith (2006) show that this behaviour is not confined to the laboratory, and so what we observe may not necessarily be an artefact of how waves behave in the laboratory. Most surprisingly, our observations (and those of Gjørund 2003 and Smith

2006) are most simply explained if we postulate that our waves are Gerstner waves, waves with closed orbits, or their finite-depth relatives. If this is true, and there is some evidence to the contrary (see §4.2), the challenge that awaits wave theoreticians is to determine how these waves are generated and how they might transfer vorticity horizontally through the fluid. However, from a purely experimental standpoint, it is clear that the majority of the existing observations match the Gerstner wave model better than they do the classical Stokes model, at least near the surface.

S. G. M. gratefully acknowledges support by ONR through grants N00014-94-0190 (monitored by Dr E. Rood) and N00014-93-1-0377 (monitored by Dr W. Patterson) and NSF through grant OCE 0117859. He also wishes to thank J. M. for his hospitality during S. G. M.'s sabbatical leave in Toulouse. We are grateful to Jerry Smith, Svein Helge Gjøsund, Jih Yih Jiang and Bob Street for sharing their observations with us. Finally, S. G. M. wishes to acknowledge that his interest in Stokes drift cancelling Eulerian flows was originally stimulated by discussions with Gene Terray who around 1990 had observed similar behaviour in unpublished experiments of his own.

Appendix

Application of the Mellor (2003, hereinafter referred to as M03) theory to waves advancing into still water extended classical radiation stress theory (Longuet-Higgins & Stewart 1962) to include vertical variations in mean flows interacting with waves. M03 derived conservation equations for mean mass and momentum including the effects of monochromatic waves using the sigma transformation of the vertical position,

$$z = \hat{\eta} + \zeta D + \tilde{s} \quad (\text{A } 1)$$

where

$$\begin{aligned} D &= \hat{\eta} + H, \\ \tilde{s} &= a \frac{\sinh(kD(1 + \zeta))}{\sinh(kD)} \cos(kx_1 - \sigma t), \end{aligned}$$

ζ varies between -1 (the bottom) and 0 (the free surface, which has the variable part $\hat{\eta}$). M03 expresses both continuity and hydrostatic momentum equations in terms of the sum of the Eulerian mean velocity and the Stokes drift velocity as

$$U_\alpha = \hat{u}_\alpha + u_{s\alpha}, \quad (\text{A } 2)$$

where $\alpha = 1, 2$ refer to the two horizontal directions. Note that $\hat{u}_\alpha = (\overline{U_E})_\alpha$, i.e. the caretted variables represent the mean flow whereas variables marked with \sim represent the waves, and variables marked with a prime represent turbulence. In terms of these variables, continuity (which includes the transformed vertical velocity Ω) is written as

$$\frac{\partial(DU_\alpha)}{\partial x_\alpha} + \frac{\partial\Omega}{\partial\zeta} + \frac{\partial\hat{\eta}}{\partial t} = 0, \quad (\text{A } 3)$$

and momentum conservation is

$$\frac{\partial(DU_\alpha)}{\partial t} + \frac{\partial(DU_\alpha U_\beta)}{\partial x_\beta} + \frac{\partial(\Omega U_\alpha)}{\partial\zeta} + gD \frac{\partial\hat{\eta}}{\partial x_\alpha} = -\frac{\partial S_{\alpha\beta}}{\partial x_\beta} + \frac{\partial(\tilde{s}_\alpha \tilde{p})}{\partial\zeta} - \frac{\partial}{\partial\zeta} \langle w' u'_\alpha \rangle, \quad (\text{A } 4)$$

where the wave interaction terms are

$$S_{\alpha\beta} = kDE \left[\frac{k_\alpha k_\beta}{k^2} F_{CS} F_{CC} + \delta_{\alpha\beta} (F_{CS} F_{CC} - F_{SS} F_{CS}) \right],$$

$$\overline{\tilde{s}_\alpha \tilde{p}} = (F_{CC} - F_{SS}) E^{1/2} \frac{\partial}{\partial x_\alpha} (E^{1/2} F_{SS}).$$

Here $E = ga^2/2$ is the energy density. M03 defines F_{CC} etc., the various functions of kD and ζ and shows that in the limit where $kD \rightarrow \infty$, they all asymptote to $\exp(kD\zeta)$, in which case

$$\left. \begin{aligned} S_{\alpha\beta} &= DE \frac{k_\alpha k_\beta}{k} \exp(2kD\zeta), \\ \overline{\tilde{s}_\alpha \tilde{p}} &= 0, \end{aligned} \right\} \quad (\text{A } 5)$$

and the momentum equations reduce to

$$\begin{aligned} \frac{\partial(DU_\alpha)}{\partial t} + \frac{\partial(DU_\alpha U_\beta)}{\partial x_\beta} + \frac{\partial(\Omega U_\alpha)}{\partial \zeta} + gD \frac{\partial \hat{\eta}}{\partial x_\alpha} \\ = - \frac{\partial}{\partial x_\beta} \left[DE \frac{k_\alpha k_\beta}{k} \exp(2kD\zeta) \right] - \frac{\partial}{\partial \zeta} \langle w' u'_\alpha \rangle. \end{aligned} \quad (\text{A } 6)$$

If we focus on the simple case of long-crested (two-dimensional) waves advancing into still water with no ambient turbulence, then

$$\frac{\partial(DU_1)}{\partial t} + \frac{\partial(DU_\beta U_1)}{\partial x_\beta} + \frac{\partial(\Omega U_1)}{\partial \zeta} + gD \frac{\partial \hat{\eta}}{\partial x_1} = - \frac{\partial}{\partial x_1} [DEk \exp(2kD\zeta)].$$

For small-amplitude waves, we can make the approximation that $D \simeq H$ and that advective momentum terms are negligible and so

$$\frac{\partial U_1}{\partial t} + g \frac{\partial \hat{\eta}}{\partial x_1} = -k \exp(2kz) \frac{\partial E}{\partial x_1}. \quad (\text{A } 7)$$

In this limit, continuity reads

$$H \frac{\partial U_1}{\partial x_1} + \frac{\partial \Omega}{\partial \zeta} + \frac{\partial \hat{\eta}}{\partial t} = 0. \quad (\text{A } 8)$$

Consider a wave front that can be described as

$$\begin{aligned} E &= E_0 \left[\frac{x_f - x}{\Delta x} \right] && \text{for } x_f - x \leq \Delta x \\ &= E_0 && \text{for } x_f - x > \Delta x, \end{aligned}$$

where $x_f = C_g t$ is the position of the leading edge of the wave front that is Δx wide. Thus,

$$\begin{aligned} \frac{\partial E}{\partial x_1} &= -\frac{E_0}{\Delta x} && \text{for } x_f - x \leq \Delta x \\ &= 0 && \text{for } x_f - x > \Delta x. \end{aligned}$$

Thus for a period of time $\Delta t = \Delta x/C_g$, the radiation stress gradient acts, so that if we integrate across the front of the wave, we find that

$$\Delta U_1 = -g \frac{\partial \hat{\eta}}{\partial x_1} \frac{\Delta x}{C_g} + \frac{g(ak)^2}{2kgC_g} \exp(2kz) = -g \frac{\Delta \bar{\eta}}{C_g} + U_s(z), \quad (\text{A } 9)$$

where $U_s(z)$ is the Stokes drift velocity associated with the constant wave amplitude existing after the front has passed. Thus, in terms of the mean Eulerian flow there is only a change in the depth-independent mean flow

$$\Delta \hat{u}_{\cdot 1} = \Delta \overline{U_E} = -g \frac{\Delta \bar{\eta}}{C_g}.$$

In a like fashion, continuity can be integrated to give

$$\Delta \bar{\eta} = \frac{C_g}{gH + C_g^2} \int_{-H}^0 U_s dz = \frac{C_g Q_s}{gH + C_g^2}$$

and thus we find that

$$\Delta \overline{U_E} = -g \frac{Q_s}{gH + C_g^2} \simeq -\frac{Q_s}{H}.$$

Thus, as found by Longuet-Higgins & Stewart (1962), the mean Eulerian flow only cancels the Stokes drift transport in an integral fashion.

REFERENCES

- ANDREWS, D. G. & MCINTYRE, M. E. 1978 An exact theory of waves on a Lagrangian mean flow. *J. Fluid Mech.* **89**, 609–646.
- BEACH EROSION BOARD 1941 A study of progressive oscillatory waves in water. *Tech. Rep. 1, Beach Erosion Board, Office of the Chief of Engineers*. US Government Printing Office, Washington DC, 39 pp.
- CHEUNG, T. K. & STREET, R. L. 1988 Turbulent layers in the water at an air–water interface. *J. Fluid Mech.* **194**, 133–151.
- COEHLO, S. 1989 The production of uniformly sheared streams by means of double gauzes in wind tunnels: a mathematical analysis. *Exps. Fluids* **8**, 25–32.
- COWEN, E. A. & MONISMITH, S. G. 1997 An hybrid digital particle tracking velocimetry technique. *Exps. Fluids* **22**, 199–211.
- COWEN, E. A., MONISMITH, S. G. & KOSEFF, J. R. 1996 Digital particle tracking measurements very near a free surface. In *Air Water Transfer. Selected Papers from the Third Intl Symp. on Air–Water Gas Transfer* (ed. B. Jähne & E. C. Monahan), pp. 135–144. Aeon.
- DEAN, R. G. & DALRYMPLE, R. A. 1991 *Water Wave Mechanics for Engineers and Scientists*, 2nd edn. World Scientific.
- GROENEWEG, J. & BATTJES, J. A. 2003 Three dimensional wave effects on a steady current. *J. Fluid Mech.* **478**, 325–343.
- GROENEWEG, J. & KLOPMAN, G. 1998 Changes of the mean velocity profiles in the combined wave–current motion described in a GLM formulation. *J. Fluid Mech.* **370**, 271–296.
- GJØSUND, S. H. 2000 Kinematics in regular and irregular waves based on a Lagrangian formulation. PhD thesis, Norwegian University of Science & Technology.
- GJØSUND, S. H. 2003 A Lagrangian model for irregular waves and wave kinematics. *J. Offshore Mech. Arctic Engng* **125**, 94–102.
- HUANG, Z. & MEI, C. C. 2003 Effects of surface waves on a turbulent current over a smooth or rough seabed. *J. Fluid Mech.* **497**, 253–287.
- JIANG, J. Y. & STREET, R. L. S. 1991 Modulated flows beneath wind-ruffled, mechanically generated waves. *J. Geophys. Res. (Oceans)* **96**, 2711–2721.
- KEMP, P. & SIMONS, R. 1982 The interaction between waves and a turbulent current: waves propagating with the current. *J. Fluid Mech.* **116**, 227–250.
- KIMMEL, S. J. 1994 Turbulent structures in a wavy flow. Engineer Degree thesis, Dept of Mech. Engng, Stanford University.
- KINSMAN, B. 1984 *Wind Waves: Their Generation and Propagation on the Ocean's Surface*. Dover.
- KLOPMAN, G. 1994 Vertical structure of flow due to waves and currents. *Prog. Rep. Delft Hydraul.* H 840.32, Part 2.

- LAMB, H. 1932 *Hydrodynamics*. Cambridge University Press.
- LAW, A. W. K. 1999 Wave-induced surface drift of an inextensible thin film. *Ocean Engng* **26**, 1145–1168.
- LEIBOVICH, S. On wave–current interaction theories of Langmuir circulations. *J. Fluid Mech.* **99**, 715–724.
- LONGUET-HIGGINS, M. S. 1953 Mass transport in water waves. *Phil. Trans. R. Soc. Lond. A* **245**, 535–581.
- LONGUET-HIGGINS, M. S. 1960 Mass transport in the boundary layer at a free oscillating surface *J. Fluid Mech.* **8**, 293–306.
- LONGUET-HIGGINS, M. S. 1992 Capillary rollers and bores. *J. Fluid Mech.* **240**, 659–679.
- LONGUET-HIGGINS, M. S. & STEWART, R. 1962 Radiation stress and mass transport in gravity waves with application to 'surf beats'. *J. Fluid Mech.* **13**, 481–504.
- MCINTYRE, M. E. 1981 On the 'wave momentum' myth. *J. Fluid Mech.* **106**, 331–347.
- MAGNAUDET, J. & MASBERNAT, L. 1990 Interaction des vagues de vent avec le courant moyen et la turbulence. *C.R. Acad. Sci. Paris* **311**, Ser. II, 1461–1466.
- MATSUNAGA, N., TAKEHARA, K., & AWAYA, Y. 1994 The offshore vortex train. *J. Fluid Mech.* **236**, 113–124.
- MELLOR, G. 2003 The three-dimensional current and surface wave equations. *J. Phys. Ocean.* **33**, 1978–1989.
- MELVILLE, W. K. 1982 The instability and breaking of deep water waves. *J. Fluid Mech.* **115**, 165–185.
- MELVILLE, W. K. 1983 Wave modulation and breakdown. *J. Fluid Mech.* **128**, 489–506.
- MONISMITH, S. G., & FONG, D. A. 2004 A note on the transport of scalars and organisms by surface waves. *Limnol. Ocean.* **49**, 1214–1219.
- MONISMITH, S. G. & MAGNAUDET, J. 1998 On wavy mean flows, strain, turbulence and Langmuir cells. *IUTAM Symp. on Physical Limnology* (ed. J. Imberger), AGU Monograph, pp. 101–110.
- NEPF, H. M. 1992 The production and mixing effects of Langmuir circulations. PhD thesis, Dept of Civil Engng, Stanford University.
- NEPF, H. M. & MONISMITH, S. G. 1994 Wave dispersion on a sheared current. *Appl. Ocean Res.* **16**, 313–315.
- NEPF, H. M., COWEN, E. A., KIMMEL, S. J. & MONISMITH, S. G. 1995 Longitudinal vortices under breaking waves. *J. Geophys. Res. (Oceans)* **100**, 16 211–16 221.
- RUSSELL, R. C. & OSORIO, J. D. C. 1958 An experimental investigation of drift profiles in a closed channel. *Proc. Sixth Conf. Coastal Engng, Florida, Dec. 1957* (ed. J. W. Johnson), pp. 171–183.
- SMITH, J. A. 2006 Wave groups, Stokes drift and Eulerian response. *J. Phys. Oceanogr.* (in press).
- STOKES, G. G. 1847 On the theory of oscillatory waves. *Trans. Camb. Phil. Soc.* **8**, 441–55.
- SWAN, C. 1990a Convection within an experimental wave flume. *J. Hydraul. Res.* **28**, 273–282.
- SWAN, C. 1990b Experimental study of waves on a strongly sheared current profile. In *Proc. 22nd Intl Coastal Engng Conf.* pp. 489–502.
- TEIXEIRA, M. A. C. & BELCHER, S. E. 2003 On the distortion of turbulence by a progressive surface wave. *J. Fluid Mech.* **458**, 229–267.
- THAIS, L. 1994 *Contribution a l'étude du mouvement turbulent sous des vagues de surface cisillées par le vent*. Thèse Inst. Nat. Polytech. de Toulouse, Toulouse.
- THAIS, L. & MAGNAUDET, J. 1996 Turbulence structure beneath surface gravity waves sheared by the wind. *J. Fluid Mech.* **328**, 313–344.
- WIEGEL, R. L. 1964 *Oceanographical Engineering*. Prentice-Hall.